DOI: 10.1002/ejoc.201101273

Looking for a Robust, Synthetic, Fully-Extended (2.0_5-Helical) Peptide Structure – Effect of Terminal Groups

Fernando Formaggio,*[a] Marco Crisma,[a] Cristina Peggion,[a] Alessandro Moretto,[a] Mariano Venanzi,[b] and Claudio Toniolo*[a]

Keywords: Amino acids / Peptides / Solution peptide synthesis / Conformation analysis

The incorporation of α-amino acids with a quaternary α-carbon atom into a peptide provides a tool to effectively restrict the available range of its backbone conformations. Specifically, under favorable conditions, $C^{\alpha,\alpha}$-diethylglycine (Deg) homopeptides are known to preferentially adopt the fully-extended (2.0_5-helical) structure, which is characterized by the longest possible separation between two adjacent α-amino acid C^{α} atoms. We have investigated the influence of the nature of the N- and/or C-terminal protecting (or blocking) groups on the relative stabilities of the fully-extended conformation vs. the competing, shorter 3_{10}-helical structure in a synthetic Deg homopeptide series.

Introduction

The fully-extended (2.0_5-helical) or planar sheet peptide structure represents an extremely appealing molecular spacer in long-range donor–acceptor studies as it is endowed with the longest distance between two consecutive α-amino acid α-carbon atoms.[1] This conformation, although proposed at an early stage in 3D-structural studies of proteins,[2] is extremely rare. Indeed, as predicted,[2] it has so far only been authenticated in the –$(Gly)_4$– sequence of His-tRNA-synthetase.[3] The twofold (2.0) repeating motif of this peptide conformation is based on the 2→2 intramolecularly H-bonded form depicted in Figure 1. The relative disposition of the two dipoles, N(2)–H(2) and C′(2)=O(2), is such that there is obviously some interaction between them.[4,5] As these four atoms, along with the α-carbon atom of the second residue, are involved in a cyclic (pentagonal) structure, this conformation is termed the C_5 structure.

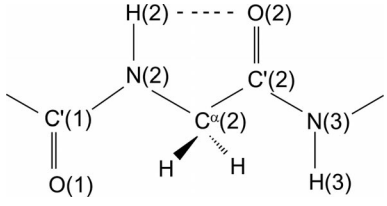

Figure 1. The 2→2 intramolecularly H-bonded (C_5) peptide conformation for a Gly residue.

Apart from protein residues, we and others have shown theoretically and experimentally that specific backbone-modified α-amino acids, e.g. $C^{\alpha,\beta}$-didehydroalanine (ΔAla)[6] (Scheme 1) and, in particular, the subclass of (achiral and chiral) $C^{\alpha,\alpha}$-dialkylated glycines with both side chains longer than methyl but not interconnected in a cyclic system,[1,7–22] typically favor a monomeric (not self-associated) fully-extended structure. The simplest member of this subclass is the achiral $C^{\alpha,\alpha}$-diethylglycine (Deg, Scheme 1). On the other hand, C^{α}-methylated, C^{α}-alkylated (methyl or longer alkyl group) α-amino acids, the prototype of which is α-aminoisobutyric acid (Aib),[7,10–13,16–19,23–26] and $C^{\alpha,\alpha}$-cyclized Gly residues (1-aminocycloalkane-1-carboxylic acids, Ac_nc)[10,16] are known to strongly prefer the much more compact 3_{10}-[27] or α-helical structures ($\phi = \pm60° \pm20°$; $\psi = \pm30° \pm15°$). However, the fully-extended conformation seems to be rather fragile as even a modest sequence modifi-

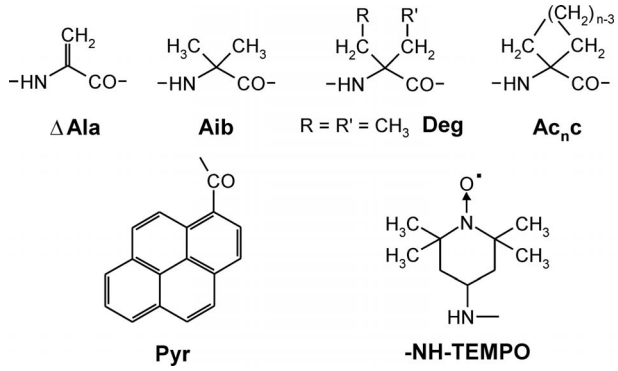

Scheme 1. Structures of the α-amino acids, Pyr and –NH–TEMPO terminal moieties discussed.

[a] ICB, Padova Unit, CNR, Department of Chemical Sciences, University of Padova,
35131 Padova, Italy
Fax: +39-049-8275829
E-mail: fernando.formaggio@unipd.it
claudio.toniolo@unipd.it
[b] Department of Chemical Sciences and Technologies, University of Rome "Tor Vergata",
00133 Rome, Italy

cation, e.g. incorporation of a single α-aminobutyric acid residue (with only one ethyl side chain) into a host $(Deg)_n$ peptide may force it into the competing 3_{10} helix.[21,28]

In search of a robust fully-extended peptide structure, we have studied the conformational effects induced by the type of *N*- and/or *C*-protecting (or blocking) groups on the relative propensities of well-characterized Deg homopeptides[29,30] (to the tetramer level) to adopt either the fully-extended or the 3_{10}-helical conformation. To this end, we utilized FTIR, 1D and 2D NMR spectroscopy, and steady-state fluorescence techniques. The results were compared with those obtained for Aib homopeptides (with the same protecting or blocking groups) used as 3_{10}-helical standards.

Results and Discussion

Synthesis

For the synthesis of the Pyr–$(Deg)_n$–NH–TEMPO homopeptide series (Pyr = 1-pyrenylcarbonyl; n = 1–4; NH–TEMPO = 4-amino-1-oxyl-2,2,6,6-tetramethylpiperidinyl, Scheme 1), we first prepared the corresponding Tfa–$(Deg)_n$–O*t*Bu (Tfa = trifluoroacetyl) peptides.[29,30] The initial procedure involves the syntheses of Tfa–Deg–OH and H–Deg–O*t*Bu (H–Deg–O*t*Bu was prepared by catalytic hydrogenation of Z–Deg–O*t*Bu,[31] Z = benzyloxycarbonyl). Throughout the series, peptide bond formation was achieved from Tfa–Deg–OH and H–$(Deg)_n$–O*t*Bu (n = 1–3) in the presence of *O*-(7-azabenzotriazol-1-yl)-1,1,3,3-tetramethyluronium (HATU) hexafluorophosphate[32,33] and *N*,*N*-diisopropylethylamine (DIEA) in anhydrous acetonitrile. Selective, reductive Tfa removal was achieved by treatment of the *N*-protected peptides with $NaBH_4$ in ethanol.[14,30]

The N-terminal Pyr moiety was introduced in the Tfa-deprotected H–$(Deg)_n$–O*t*Bu (n = 1–4) peptides by 1-pyrenylcarboxylic acid in the presence of HATU/DIEA in anhydrous dichloromethane. The Pyr-protected peptide free acids were synthesized from the corresponding *tert*-butyl esters in trifluoroacetic acid (TFA)/dichloromethane (1:1). Finally, the target Pyr–$(Deg)_n$–NH–TEMPO (n = 1–4) homopeptides were obtained from the corresponding free acids and NH_2-TEMPO as described above for the corresponding Pyr-protected peptide *tert*-butyl esters.

Syntheses of the known Z–$(Aib)_n$–O*t*Bu (n = 1–5) homopeptides[34,35] were performed either by the 1-(3-dimethylamino)propyl-3-ethylcarbodiimide (EDC)/7-aza-1-hydroxy-1,2,3-benzotriazole (HOAt) method to activate Z–Aib–OH in anhydrous dichloromethane with *N*-methylmorpholine (for the dimer and trimer) or via the intermediate 5(4*H*)-oxazolone from Z–$(Aib)_2$–OH[31,34–37] in anhydrous CH_3CN under reflux (for the tetramer and pentamer). This oxazolone was, in turn, prepared by treatment of the N^{α}-protected dipeptide free acid with EDC in anhydrous CH_3CN. The Pyr–$(Aib)_n$–O*t*Bu and Pyr–$(Aib)_n$–NH–TEMPO (n = 1–5) series were synthesized from the corresponding Z–$(Aib)_n$–O*t*Bu and Pyr–$(Aib)_n$–OH oligomers, respectively, as described for the $(Deg)_n$ series.

Solution Conformational Analysis

The preferred solution conformations of the Pyr–$(Deg)_n$–NH–TEMPO (O*t*Bu) oligopeptides were investigated and compared with those of the corresponding $(Aib)_n$ compounds by FTIR and NMR spectroscopy.

The FTIR spectra in the conformationally informative N–H stretching region (3500–3200 cm^{-1}) of the Pyr-blocked $(Deg)_n$ and $(Aib)_n$ homooligopeptide series to the tetramer and pentamer levels, respectively, are shown in Figure 2. Above 3400 cm^{-1}, the two Aib series (Figure 2, A and B) exhibit one (or two) bands associated with the free (solvated) N–H vibrations.[4,38,39] Below 3400 cm^{-1}, a strong band is seen at 3368 cm^{-1} in the trimer ester, and at 3346 cm^{-1} in the dimer amide, which are associated with H-bonded N–H vibrations.[4,38,39] Both bands significantly shift to lower wavenumbers (to 3348 and 3328 cm^{-1}, respectively) and their relative intensities markedly and linearly increase upon main-chain elongation. The spectra do not change in the concentration range investigated (10.0–0.1 mM, not shown), which strongly supports the view that the observed H-bonding is intramolecular. These results, which match those reported for the Z-protected $(Aib)_n$ series,[40] are typical of a 3_{10} helix, which is cooperatively stabilized with increasing backbone length.

The FTIR spectra of the Pyr–$(Deg)_n$–O*t*Bu oligomers (Figure 2, C) are significantly different from those of the $(Aib)_n$ series discussed above. In particular, an intense absorption at 3395 cm^{-1} occurs at the monomer level. This band is assigned to the C-terminal conformer II (Scheme 2), where the H-bonding acceptor of the C_5 structure is the ester carbonyl oxygen atom.[41] The amount of free (solvated) N–H stretching vibrations (a weak band at about 3440 cm^{-1}) is very low. Upon main-chain elongation to dimer, trimer, and tetramer, an absorption appears at the lower frequency of 3364 cm^{-1}. The position of this band does not change from dimer to tetramer. Again, a variation of the peptide concentration modifies the spectra only slightly. This general behavior, which is in good agreement with that of the Tfa-protected Deg,[9] Beg (C^{α}-*n*-butyl, C^{α}-ethylglycine),[42] and Epg (C^{α}-ethyl, C^{α}-*n*-pentylglycine)[41] series, is attributed to an ever increasing contribution of the C_5 internal conformer I (Scheme 2).

The FTIR spectra of the Pyr–$(Deg)_n$–NH–TEMPO series (Figure 2, D) provide evidence for somewhat intermediate behavior between those of the $(Aib)_n$ and $(Deg)_n$ ester series. Based on a comparison between the spectra of Pyr–NH–TEMPO and Pyr–$(Deg)_2$–O*t*Bu, the two bands in the spectrum of the monopeptide Pyr–Deg–NH–TEMPO at 3438 and 3374 cm^{-1} are assigned to the free NH group of the –NH–TEMPO moiety and the C_5 H-bonded NH group of Deg, respectively. In the spectrum of the Deg dipeptide amide, an additional shoulder is seen near 3345 cm^{-1}. This band, more clearly observed in the spectrum of the corresponding Aib dipeptide amide (Figure 2, B), is assigned to an intramolecularly H-bonded, folded C_{10} (β-turn) conformer, which is the basic unit of a 3_{10} helix.[27] Elongation of the peptide backbone in this Deg series generated spectra

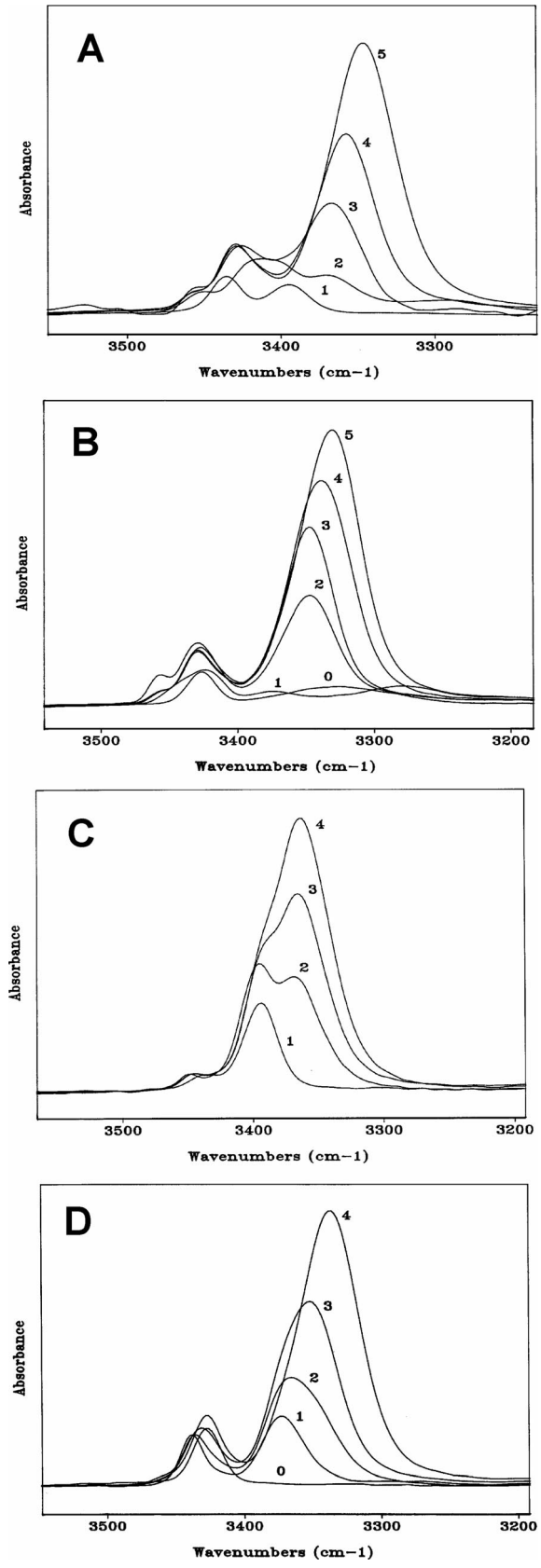

Figure 2. FTIR spectra (3550–3200 cm^{-1}) of (A) Pyr–$(Aib)_n$–O*t*Bu (n = 1–5), (B) Pyr–$(Aib)_n$–NH–TEMPO (n = 1–5), (C) Pyr–$(Deg)_n$–O*t*Bu (n = 1–4), and (D) Pyr–$(Deg)_n$–NH–TEMPO (n = 0–4) in $CDCl_3$ (peptide concentration: 1 mM).

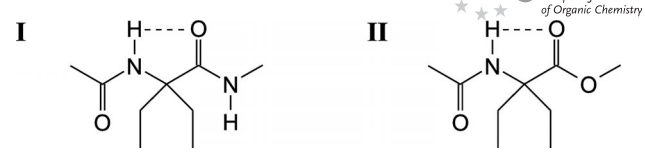

Scheme 2. The C_5 internal (I) and C-terminal (II) conformers of the Deg homopeptides.

that tend towards those of the corresponding 3_{10}-helical Aib peptide series with a predominant band near 3340 cm^{-1} and an increasingly less intense shoulder near 3370 cm^{-1}. Peptide concentration does not significantly affect the spectra.

Looking at all the FTIR data, we conclude that a C-terminal secondary amide offers the Deg peptide series a chance to fold in a 3_{10} helix where the starting point is provided by the H-bond donor –NH–TEMPO group. The position of this conformational equilibrium is shifted from the C_5 conformation to the 3_{10} helix as the peptide backbone is elongated to the tetramer level. Contrary to the behavior of the Pyr-blocked Deg peptide esters, this phenomenon makes the preferred conformation of the longer Deg peptide amides more similar to that of the corresponding Aib amide peptides.[20]

More detailed information on the secondary structural propensities of the Pyr-blocked Deg homooligopeptide esters was extracted from 1D and 2D NMR spectra. The NH proton resonances were assigned from the NH(i)→NH(i+1) space connectivities obtained from 2D ROESY experiments[43,44] and a comparison with those of the corresponding Tfa-protected analogs[9] in the same solvent. A section of the ROESY spectrum of the Deg trimer is illustrated in part B of Figure 3. The NH(1) chemical shifts of the Pyr-blocked and Tfa-protected homotrimers reveal a slight conformational change at the N-terminus. Indeed, this backbone region is more rigid in the Tfa-protected compound by virtue of three-center F···H···O H-bonding (missing in the Pyr peptide), which is reflected in a shift to lower field (ca. 8.0 ppm) of the Tfa-NH proton[9] compared to about 7.6 ppm for the Pyr-NH proton. This investigation was conducted in parallel with a study of the related $(Aib)_n$ oligomers (the ROESY spectrum of the pentapeptide is shown in part A of Figure 3).

First, we performed a solvent titration of the NH proton chemical shifts; as an example, those of the –$(Deg)_4$– ester are reported in Figure 4 in comparison with those of the –$(Aib)_4$– ester. The polar solvent dimethyl sulfoxide (DMSO)[45] added to the $CDCl_3$ solution is expected to interact strongly with the exposed (not intramolecularly H-bonded) peptide/amide NH protons through N–H···O=S H-bond formation, which would induce a downfield shift in their resonances.[46] Interestingly, only one class of NH protons is observed in each of the four Deg homooligomers, and all the NH proton chemical shifts are only slightly sensitive to the presence of the perturbing solvent. The lack of solvent accessibility is compatible with the occurrence of the fully-extended conformation in $CDCl_3$ solution for these compounds. These results are at variance with those

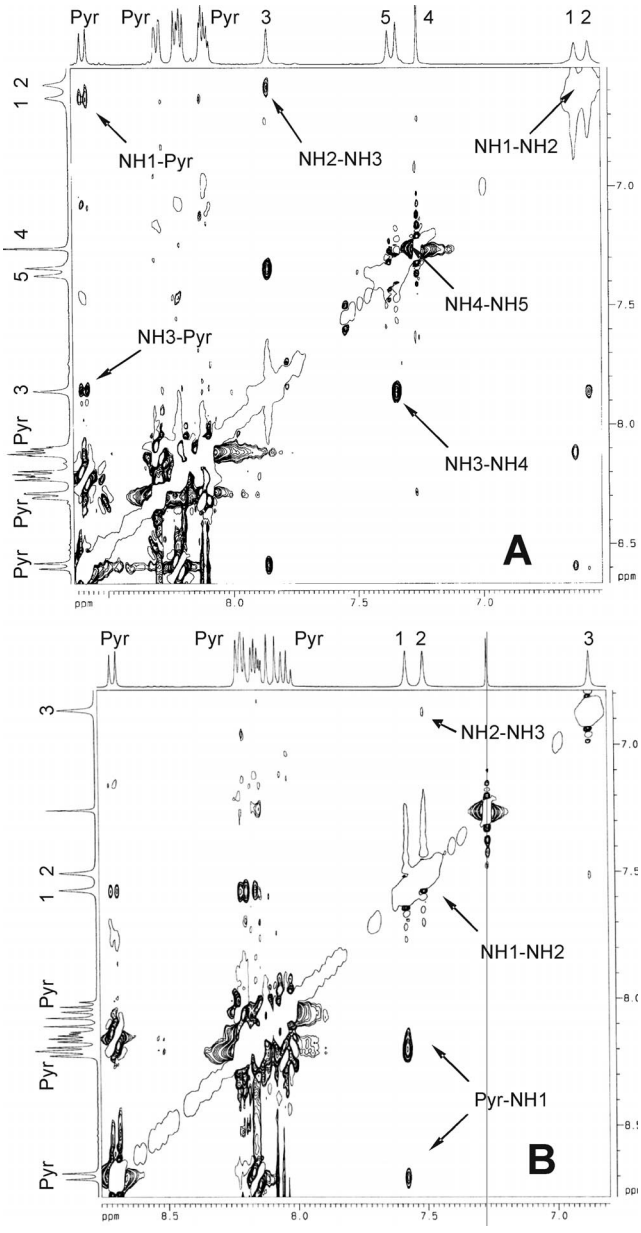

Figure 3. Sections of the ROESY spectra of (A) Pyr–$(Aib)_5$–O*t*Bu and (B) Pyr–$(Deg)_3$–O*t*Bu in $CDCl_3$ solution (peptide concentration: 10 mM). The NH(*i*)→NH(*i*+1) and Pyr→NH1 cross-peaks are indicated.

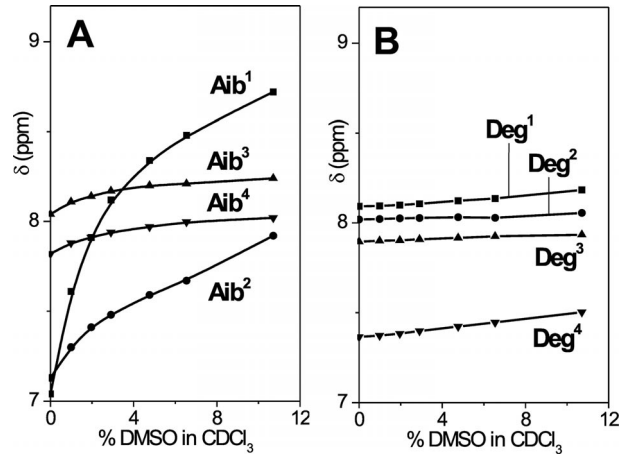

Figure 4. Plots of the NH proton chemical shifts in the ^1H NMR spectra of (A) Pyr–$(Aib)_4$–O*t*Bu and (B) Pyr–$(Deg)_4$–O*t*Bu as a function of the increasing amount of DMSO added to the $CDCl_3$ solution (*v*/*v*) (peptide concentration: 1 mM).

of the $(Aib)_n$ (n = 1–5) oligomers, where two classes of NH proton chemical shifts were observed. The first class (encompassing the first and second NH groups, numbering the residues from the N-terminus) includes NH protons that are very sensitive to DMSO, whereas the second class (all other NHs) includes NH protons that are marginally sensitive to DMSO. Therefore, we propose that the $(Aib)_n$ oligomers adopt the 3_{10} helix where the H-bonding donor NH groups are those of the third, fourth, and fifth residues.

The ROESY spectra of the $(Deg)_n$ and $(Aib)_n$ oligopeptides (Figure 3) differ in several aspects. In the spectrum of the –$(Aib)_5$– oligomer, all NH(*i*)→NH(*i*+1) cross-peaks are clearly observed. This finding strongly supports the view that this peptide is highly folded. Two other 3D-structurally informative cross-peaks involve a Pyr aromatic proton and either the Aib^1 or the Aib^3 NH proton. This connectivity indicates the onset of a helical structure. Analogous data were found for the shorter $(Aib)_n$ oligomers. In contrast, in the spectrum of the –$(Deg)_3$–oligomer, all NH(*i*)→NH(*i*+1) cross-peaks are extremely weak (similar findings were obtained for the Tfa-protected Deg homo-oligomers). In addition, a Pyr aromatic proton interacts with the Deg^1 NH proton but not with the other two NH protons in this compound. A different ROESY section of the Pyr-blocked –$(Deg)_3$– spectrum (not shown) emphasizes the occurrence of cross-peaks between the NH(*i*) protons and the $C^{\beta}H_2$ (and $C^{\gamma}H_3$) protons of the preceding (*i*–1) residue. Again, this spatial vicinity is compatible with the presence of a fully-extended conformation. In summary, our FTIR and NMR spectroscopic studies show that the preferred conformation of the Pyr-blocked $(Deg)_n$ and $(Aib)_n$ oligomer esters is remarkably different; the $(Aib)_n$ peptides fold in a 3_{10} helix,[20] whereas the $(Deg)_n$ peptides prefer the fully-extended structure.

Molecular Spacers

The fully-extended peptide conformation is extremely promising as a molecular spacer in spectroscopic analysis. We utilized this secondary structure in a steady-state fluorescence study. To this end, we incorporated the Pyr photosensitizer group[47,48] at the N-terminus of the backbone and the paramagnetic, free radical quencher –NH–TEMPO[49,50] moiety at the C-terminus. The quenching phenomenon is explained in terms of an intramolecular effect, as no intermolecular quenching is observed in the highly diluted peptide solution (10^{-7} M in MeOH). Moreover, negligible quenching was seen in a 1:1 mixture of Pyr–Deg–O*t*Bu and CH_3–CONH–TEMPO at the same concentration. The Pyr–NH···CONH–TEMPO donor···acceptor distance is believed to play a major role in these experi-

ments, and the pyrenyl···nitroxide relative orientation may exert some effect as well.[48]

Figure 5 (A and B) shows the steady-state fluorescence spectra of the Pyr–$(Aib)_n$–NH–TEMPO (n = 0–4) and the Pyr–$(Deg)_n$–NH–TEMPO (n = 0–4) series, respectively. Spectra of the reference compounds Pyr–$(Aib)_4$–O*t*Bu and Pyr–$(Deg)_4$–O*t*Bu are also shown. Figure 5 and Table 1, which lists the percentages of fluorescence quenching in peptides of different lengths, indicate that the trend is similar for both series.

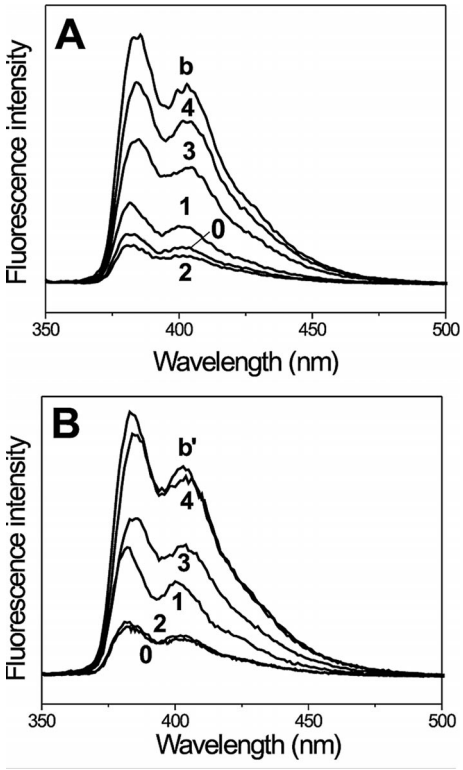

Figure 5. Steady-state fluorescence spectra of (A) Pyr–$(Aib)_4$–O*t*Bu (blank b) and Pyr–$(Aib)_n$–NH–TEMPO (n = 0–4), and (B) Pyr–$(Deg)_4$–O*t*Bu (blank b′) and Pyr–$(Deg)_n$–NH–TEMPO (n = 0–4) in MeOH (peptide concentration: 10^{-7} M; λ_{exc} = 340 nm).

Table 1. Extent of fluorescence quenching observed for Pyr–NH–TEMPO (n = 0, reference), Pyr–$(Aib)_n$–NH–TEMPO (n = 1–4) and Pyr–$(Deg)_n$–NH–TEMPO (n = 1–4).

n	Pyr–$(Aib)_n$–NH–TEMPO [%]	Pyr–$(Deg)_n$–NH–TEMPO [%]
0	80	80
1	68	51
2	84	79
3	42	40
4	20	12

Specifically, the extent of quenching decreases with the increasing number of spacer units with the remarkable exception of the two Pyr–$(X)_2$–NH–TEMPO (X = Aib, Deg) peptides, which exhibit a quenching efficiency as high as that of the quencher derivative (n = 0). This finding supports the view that both peptide series are highly folded in the 3_{10}-helical conformation because the fluorophore and quencher groups are expected to be spatially close in the n = 2 compounds in this threefold 3D-structure. This conclusion is in agreement with the FTIR spectroscopic results discussed above for the same two peptide series. For both series the amount of fluorescence surviving in the tetrapeptide amide is significantly high (80–90%). The extent of quenching is less significant for the Deg series relative to its Aib counterpart. This is consistent with a mixture of predominantly 3_{10}-helices with a high amount of the fully-extended conformation in the Deg peptides, whereas the fully-extended conformer is absent in the Aib peptides (the fluorophore···quencher separation is longer in the fully-extended conformation).

Conclusions

Over the last 25 years, the highly crystalline nature of peptides rich in C^{α}-tetrasubstituted residues has been exploited to characterize the fully-extended (C_5) conformation and the related 2.0_5 helix by X-ray diffraction. In particular, multiple, consecutive C_5 conformations have been observed in homopeptides with two side chains longer than methyl,[10,11,14,16,18,19,41,42] which is the case for achiral Deg. Further evidence for this conclusion has come from spectroscopic studies in solution and conformational energy computations. Interestingly, the axial translation per residue in the 2.0_5 helix is about 3.80 Å, the longest possible for a single amino acid, which makes this conformation extremely attractive to use as a spacer or bridge. However, we[21,28] and Tanaka et al.[14] have found that this type of helical structure is not very robust, as subtle perturbations in the chemical structure and environment can induce a dramatic conformational switch to the 40% shorter 3_{10} helix.

In this work, with the aim of detecting the most appropriate chemical structures for the stabilization of the 2.0_5 helix, we synthesized and characterized several Deg homopeptides (to the tetramer level), which differ in the nature of the N- and/or C-terminal protecting (or blocking) groups, and compared them to the corresponding Aib homopeptides, which represent classical model 3_{10} helices. Our present and published findings, combined with those of Tanaka et al.,[14] led us to conclude that:

(i) The N-terminal group most suitable for stabilizing the 2.0_5 helix is Tfa, thanks to its ability to generate an additional intramolecular F···H–N H-bond at the N-terminus. However, other amides (including Pyr) or urethane N-terminal groups may accomplish a similar role, at least in a low polarity solvent ($CHCl_3$).

(ii) Any ester (but especially a *tert*-butyl ester) group at the C-terminus is compatible with the 2.0_5 helix. Conversely, a secondary amide induces the formation of a 3_{10} helix, particularly in homologs to the tetramer level, because of its extra H-bonding donor NH group, which is unsatisfied in the 2.0_5 helix.

(iii) The absence or nature of the solvent is crucial in governing the Deg homopeptide conformation. In particu-

lar, crystal-packing forces and the type of crystallization solvent may induce a 3_{10}-helical structure in a peptide that is fully extended in $CDCl_3$. However, in general, only limited and scattered information is available on the role of the solvent on this conformational equilibrium. It is evident that this phenomenon deserves a more detailed investigation, which is currently in progress in our laboratories.

Experimental Section

Synthesis and Characterization: Materials and reagents were of the highest commercially available grade and used without further purification. Melting points were determined in open capillaries with a Leitz Laborlux 12 apparatus. Solid-state IR spectra (KBr disk) were recorded with a Perkin–Elmer model 1720X FTIR spectrophotometer. TLC was performed with Merck Kieselgel 60F_{254} precoated plates using the following solvent systems: (1) chloroform/ethanol, 9:1; (2) 1-butanol/acetic acid/water, 3:1:1; and (3) toluene/ethanol, 7:1. The chromatograms were visualized by UV fluorescence or developed by chlorine/starch/potassium iodide or ninhydrin chromatic reaction as appropriate. All compounds were obtained in a chromatographically homogeneous state. Flash chromatography was carried out with Merck silica gel 60 (40–63 μm mesh). MS (ESI mode) were measured with a Perseptive Biosystems (Mariner model) ESI-TOF spectrometer.

General Procedure for the Coupling Reaction between Pyr–(X)$_n$–OH (C component) and H–(X)$_n$–O*t*Bu (X = Deg or Aib) or NH$_2$-TEMPO (N component): To a solution of the C component (0.80 mmol) in anhydrous CH_2Cl_2 at 0 °C were added HATU (0.83 mmol) and DIEA (0.83 mmol). After 10 min, the N-component (0.80 mmol) was added. The resulting solution was heated to reflux for 4–7 d with stirring. The solvent was evaporated under reduced pressure and EtOAc was added. The organic phase was washed with 10% $KHSO_4$, H_2O, 5% $NaHCO_3$, and water and dried with Na_2SO_4. The solution was filtered, and the solvent was evaporated under reduced pressure. The product was purified using flash chromatography and an appropriate CH_2Cl_2/ethanol mixture as eluant.

General Procedure for the Removal of the *tert*-Butyl Ester *C* Protection: The *C*-protected peptide was dissolved in TFA/anhydrous CH_2Cl_2 (1:1) and the solution was stirred at room temperature for 30 min. The solvent mixture was evaporated under reduced pressure and the product was repeatedly triturated with diethyl ether to remove the remaining TFA. The product was collected by filtration and dried with KOH in a dessiccator under vacuum.

Pyr–Deg–O*t*Bu: Yield 75%; m.p. 121–122 °C [from EtOAc/petroleum ether (PE)]. R_f1 = 0.95; R_f2 = 0.95; R_f3 = 0.80. ^{1}H NMR (400 MHz, $CDCl_3$): δ = 8.66 (d, 1 H, Pyr CH), 8.24–8.03 (m, 8 H, Pyr 8 × CH), 7.13 (s, 1 H, NH), 2.83 (qd, 2 H, 1 β-CH_2), 2.00 (qd, 2 H, 1 β-CH_2), 1.48 (s, 9 H, O*t*Bu 3 × CH_3), 0.99 (t, 6 H, 2 γ-CH_3) ppm. IR (KBr): $\tilde{\nu}$ = 3387, 1723, 1652 cm^{-1}.

Pyr–(Deg)$_2$–O*t*Bu: Yield 49%; m.p. 117–118 °C (from EtOAc/PE). R_f1 = 0.95; R_f2 = 0.95; R_f3 = 0.75. ^{1}H NMR (400 MHz, $CDCl_3$): δ = 8.69 (d, 1 H, Pyr CH), 8.23–8.04 (m, 8 H, Pyr 8 × CH), 7.56 (s, 1 H, NH^1), 7.00 (s, 1 H, NH^2), 3.02 (qd, 2 H, 1 β-CH_2^1), 2.49 (qd, 2 H, 1 β-CH_2^2),1.88 (qd, 2 H, 1 β-CH_2^1), 1.78 (qd, 2 H, 1 β-CH_2^2), 1.53 (s, 9 H, O*t*Bu 3 × CH_3), 1.06 (t, 6 H, 2 γ-CH_3^1), 0.81 (t, 6 H, 2 γ-CH_3^2) ppm. IR (KBr): $\tilde{\nu}$ = 3394, 3360, 3311, 1734, 1650 cm^{-1}.

Pyr–(Deg)$_3$–O*t*Bu: Yield 58%; m.p. 200–201 °C (from CH_2Cl_2/PE). R_f1 = 0.95; R_f2 = 0.95; R_f3 = 0.70. ^{1}H NMR (400 MHz, $CDCl_3$): δ = 8.70 (d, 1 H, Pyr CH), 8.23–8.03 (m, 8 H, Pyr 8 × CH), 7.58 (s, 1 H, NH^1), 7.51 (s, 1 H, NH^2), 6.87 (s, 1 H, NH^3), 2.94 (qd, 2 H, 1 β-CH_2^1), 2.68 (qd, 2 H, 1 β-CH_2^2), 2.47 (qd, 2 H, 1 β-CH_2^3), 1.93 (qd, 2 H, 1 β-CH_2^1), 1.80 (qd, 2 H, 1 β-CH_2^3), 1.68 (qd, 2 H, 1 β-CH_2^2), 1.50 (s, 9 H, O*t*Bu 3 × CH_3), 1.06 (t, 6 H, 2 γ-CH_3^1), 0.88 (t, 6 H, 2 γ-CH_3^2), 0.81 (t, 6 H, 2 γ-CH_3^3) ppm. IR (KBr): $\tilde{\nu}$ = 3394, 3377, 3353, 1721, 1676, 1649 cm^{-1}.

Pyr–(Deg)$_4$–O*t*Bu: Yield 47%; m.p. 205–206 °C (from EtOAc/PE). R_f1 = 0.95; R_f2 = 0.95; R_f3 = 0.60. ^{1}H NMR (400 MHz, $CDCl_3$): δ = 8.70 (d, 1 H, Pyr CH), 8.23–8.03 (m, 8 H, Pyr 8 × CH), 7.59 (s, 1 H, NH^1), 7.52 (s, 1 H, NH^2), 7.40 (s, 1 H, NH^3), 6.86 (s, 1 H, NH^4), 3.0 (qd, 2 H, 1 β-CH_2^1), 2.66 (m, 4 H, 1 β-CH_2^2, 1 β-CH_2^3), 2.44 (qd, 2 H, 1 β-CH_2^4), 1.94 (qd, 2 H, 1 β-CH_2^1), 1.79–1.71 (m, 6 H, 1 β-$CH_2^2$1 β-$CH_2^3$1 β-CH2^4), 1.50 (s, 9 H, O*t*Bu 3 × CH_3), 1.06 (t, 6 H, 2 γ-CH_3^1), 0.87 (m, 12 H, 2 γ-CH_3^2 and 2 γ-CH_3^3), 0.78 (t, 6 H, 2 γ-CH_3^4) ppm. IR (KBr): $\tilde{\nu}$ = 3401, 3358, 1720, 1679, 1653 cm^{-1}.

Pyr–Deg–OH: Yield 85%; m.p. 244–245 °C. R_f1 = 0.95; R_f2 = 0.95; R_f3 = 0.15. ^{1}H NMR (400 MHz, DMSO): δ = 8.37–8.12 (m, 9 H, Pyr CH), 2.04 (m, 4 H, 2 β-CH_2), 0.91 (t, 6 H, 2 γ-CH_3) ppm. IR (KBr): $\tilde{\nu}$ = 3379, 1717, 1615 cm^{-1}.

Pyr–(Deg)$_2$–OH: Yield 98%; m.p. 234–235 °C. R_f1 = 0.95; R_f2 = 0.95; R_f3 = 0.15. ^{1}H NMR (400 MHz, DMSO): δ = 8.17–8.09 (m, 9 H, Pyr CH), 7.57 (s, 1 H, NH), 7.01 (s, 1 H, NH), 2.29 (m, 6 H, 2 β-CH_2^1 and 1 β-CH_2^2),1.87 (qd, 2 H, 1 β-CH_2^2), 1.07 (t, 6 H, 2 γ-CH_3^1), 0.82 (t, 6 H, 2 γ-CH_3^2) ppm. IR (KBr): $\tilde{\nu}$ = 3400, 3347, 3291, 1712, 1658, 1632 cm^{-1}.

Pyr–(Deg)$_3$–OH: Yield 86%; m.p. 224–225 °C. R_f1 = 0.95; R_f2 = 0.95; R_f3 = 0.10. IR (KBr): $\tilde{\nu}$ = 3383, 3341, 1724, 1676, 1659 cm^{-1}.

Pyr–(Deg)$_4$–OH: Yield 91%; m.p. 213–214 °C. R_f1 = 0.95; R_f2 = 0.95; R_f3 = 0.10. ^{1}H NMR (400 MHz, DMSO): δ = 8.59 (d, 1 H, Pyr CH), 8.37–8.12 (m, 8 H, Pyr 8 × CH), 8.53, 7.96, 7.58, 7.47 (4s, 4 H, 4 NH), 1.98 (qd, 2 H, 1 β-CH_2), 1.95–1.84 (m, 14 H, 7 β-CH_2), 1.17–0.71 (m, 24 H, 8 γ-CH_3) ppm. IR (KBr): $\tilde{\nu}$ = 3421, 1738, 1653, 1639 cm^{-1}.

Pyr–NH–TEMPO: Yield 51%; m.p. 202–203 °C (from EtOAc/PE). R_f1 = 0.90; R_f2 = 0.95; R_f3 = 0.35. IR (KBr): $\tilde{\nu}$ = 3470, 3269, 1737, 1635 cm^{-1}. MS (ESI-TOF): *m*/*z* = 401.23 [M + H]$^+$.

Pyr–Deg–NH–TEMPO: Yield 63%; m.p. 246–247 °C (from CH_2Cl_2/PE). R_f1 = 0.95; R_f2 = 0.95; R_f3 = 0.35. MS (ESI-TOF): *m*/*z* = 513.32 [M + H]$^+$.

Pyr–(Deg)$_2$–NH–TEMPO: Yield 81%; m.p. 242–243 °C (from CH_2Cl_2/PE). R_f1 = 0.70; R_f2 = 0.95; R_f3 = 0.25. IR (KBr): $\tilde{\nu}$ = 3430, 3346, 3318, 1672, 1653, 1633 cm^{-1}. MS (ESI-TOF): *m*/*z* = 626.41 [M + H]$^+$.

Pyr–(Deg)$_3$–NH–TEMPO: Yield 58%; m.p. 247–248 °C (from CH_2Cl_2/PE). R_f1 = 0.70; R_f2 = 0.95; R_f3 = 0.20. IR (KBr): $\tilde{\nu}$ = 3330, 1631 cm^{-1}. MS (ESI-TOF): *m*/*z* = 739.35 [M + H]$^+$.

Pyr–(Deg)$_4$–NH–TEMPO: Yield 80%; m.p. 251–252 °C (from CH_2Cl_2/PE). R_f1 = 0.70; R_f2 = 0.95; R_f3 = 0.15. IR (KBr): $\tilde{\nu}$ = 3429, 3327, 1652 cm^{-1}. MS (ESI-TOF): *m*/*z* = 853.32 [M + H]$^+$.

Pyr–Aib–O*t*Bu: Yield 86%; m.p. 117–118 °C (from EtOAc/PE). R_f1 = 0.90; R_f2 = 0.90; R_f3 = 0.65. ^{1}H NMR (400 MHz, $CDCl_3$): δ = 8.65 (d, 1 H, Pyr CH), 8.23 (d, 2 H, Pyr 2 × CH), 8.14 (m, 3 H, Pyr 3 × CH), 8.05 (m, 3 H, Pyr 3 × CH), 6.72 (s, 1 H, NH), 1.78 (s, 6 H, 2 β-CH_3), 1.56 (s, 9 H, O*t*Bu 3 × CH_3) ppm. IR (KBr): $\tilde{\nu}$ = 3323, 1725, 1624 cm^{-1}.

Pyr–(Aib)$_2$–O*t*Bu: Yield 95%; m.p. 210–211 °C (from EtOAc/PE). R_f1 = 0.85; R_f2 = 0.95; R_f3 = 0.35. ^{1}H NMR (400 MHz, $CDCl_3$):

δ = 8.59 (d, 1 H, Pyr 1 CH), 8.21 (d, 2 H, Pyr 2 × CH), 8.11 (m, 3 H, Pyr 3 × CH), 8.03 (m, 3 H, Pyr 3 × CH), 7.33 (s, 1 H, NH), 6.88 (s, 1 H, NH), 1.84 (s, 6 H, 2 β-CH_3), 1.63 (s, 6 H, 2 β-CH_3), 1.48 (s, 9 H, O*t*Bu 3 × CH_3) ppm. IR (KBr): $\tilde{\nu}$ = 3373, 3358, 1712, 1666, 1649 cm^{-1}.

Pyr–(Aib)$_3$–O*t*Bu: Yield 85%; m.p. 201–202 °C (from CH_2Cl_2/PE). R_f1 = 0.60; R_f2 = 0.95; R_f3 = 0.30. ^{1}H NMR (400 MHz, $CDCl_3$): δ = (d, 1 H, Pyr CH), 8.22 (d, 2 H, Pyr 2 × CH), 8.13 (m, 3 H, Pyr 3 × CH), 8.08 (m, 3 H, Pyr 3 × CH), 7.42 (s, 1 H, NH^3), 6.87 (s, 1 H, NH^2), 6.83 (s, 1 H, NH^1), 1.75 (s, 6 H, 2 β-CH_3), 1.59 (s, 6 H, 2 β-CH_3), 1.51 (s, 6 H, 2 β-CH_3) ppm. IR (KBr): $\tilde{\nu}$ = 3412, 3335, 1735, 1668, 1650 cm^{-1}.

Pyr–(Aib)$_4$–O*t*Bu: Yield 52%; m.p. 236–237 °C. R_f1 = 0.50; R_f2 = 0.95; R_f3 = 0.15. ^{1}H NMR (400 MHz, $CDCl_3$): δ = 8.59–8.62 (d, 1 H, Pyr CH), 8.28–8.30 (d, 2 H, Pyr 2 × CH), 8.18–8.23 (m, 3 H, Pyr 3 × CH), 8.09–8.12 (m, 3 H, Pyr 3 × CH), 7.56 (s, 1 H, NH^3), 7.33 (s, 1 H, NH^4), 6.63 (s, 1 H, NH^2), 6.59 (s, 1 H, NH^1), 1.75 (s, 6 H, 2 β-$CH_3{}^1$), 1.55 (s, 12 H, 2 β-$CH3^2$ and 2 β-$CH_3{}^3$), 1.52 (s, 6 H, 2 β-$CH_3{}^4$), 1.39 (s, 9 H, O*t*Bu 3 × CH_3) ppm. IR (KBr): $\tilde{\nu}$ = 3340, 1730, 1661, 1641 cm^{-1}.

Pyr–(Aib)$_5$–O*t*Bu: Yield 40%; m.p. 253–254 °C. R_f1 = 0.45; R_f2 = 0.95; R_f3 = 0.15. ^{1}H NMR (400 MHz, $CDCl_3$): δ = 8.58–8.60 (d, 1 H, Pyr CH), 8.28–8.33 (d, 2 H, Pyr 2 × CH), 8.19–8.23 (m, 3 H, Pyr 3 × CH), 8.09–8.13 (m, 3 H, Pyr 3 × CH), 7.86 (s, 1 H, NH^3), 7.37 (s, 1 H, NH^5), 7.34 (s, 1 H, NH^4), 6.63 (s, 1 H, NH^1), 6.58 (s, 1 H, NH^2), 1.74 (s, 6 H, 2 β-$CH_3{}^1$), 1.56 (s, 12 H, 2 β-$CH_3{}^2$ and 2 β-$CH_3{}^4$), 1.50 (s, 12 H, 2 β-$CH_3{}^3$, 2 β-$CH_3{}^5$), 1.44 (s, 9 H, O*t*Bu 3 × CH_3) ppm. IR (KBr): $\tilde{\nu}$ = 3331, 1734, 1662 cm^{-1}.

Pyr–Aib–OH: Yield 87%; m.p. 243–244 °C. R_f1 = 0.25; R_f2 = 0.95; R_f3 = 0.05. ^{1}H NMR (400 MHz, DMSO): δ = 8.94 (s, 1 H, NH), 8.52 (d, 1 H, Pyr CH), 8.37 (d, 2 H, Pyr 2 × CH), 8.35–8.06 (m, 6 H, Pyr 6 × CH), 1.55 (s, 6 H, 2 β-CH_3) ppm. IR (KBr): $\tilde{\nu}$ = 3329, 1705, 1632 cm^{-1}.

Pyr–(Aib)$_2$–OH: Yield 98%; m.p. 160–161 °C. R_f1 = 0.20; R_f2 = 0.90; R_f3 = 0.10. ^{1}H NMR (400 MHz, DMSO): δ = 8.49 (d, 1 H, Pyr CH), 8.17 (d, 2 H, Pyr 2 × CH), 8.06 (m, 3 H, Pyr 3 × CH), 7.97 (m, 3 H, Pyr 3 × CH), 7.72 (s, 1 H, NH), 6.79 (s, 1 H, NH), 1.78 (s, 6 H, 2 β-CH_3), 1.64 (s, 6 H, 2 β-CH_3) ppm. IR (KBr): $\tilde{\nu}$ = 3357, 3299, 1739, 1663, 1629 cm^{-1}.

Pyr–(Aib)$_3$–OH: Yield 71%; m.p. 225–226 °C. R_f1 = 0.10; R_f2 = 0.85; R_f3 = 0.10. ^{1}H NMR (400 MHz, DMSO): δ = 8.90 (s, 1 H, NH), 8.60–8.51 (d, 1 H, Pyr CH), 8.41–8.08 (m, 8 H, Pyr 8 × CH), 7.85 (s, 1 H, NH), 7.73 (s, 1 H, NH), 1.54 (s, 6 H, 2 β-CH_3), 1.42 (s, 6 H, 2 β-CH_3), 1.36 (s, 6 H, 2 β-CH_3) ppm. IR (KBr): $\tilde{\nu}$ = 3410, 3292, 1726, 1657, 1636 cm^{-1}.

Pyr–(Aib)$_4$–OH: Yield 98%; m.p. 232–233 °C. R_f1 = 0.10; R_f2 = 0.85; R_f3 = 0.10. ^{1}H NMR (400 MHz, DMSO): δ = 9.09 (s, 1 H, NH), 8.51–8.55 (d, 1 H, Pyr CH), 8.34–8.38 (d, 2 H, Pyr 2 × CH), 8.31 (s, 1 H, NH), 8.25–8.26 (m, 3 H, Pyr 3 × CH), 8.08–8.16 (m, 3 H, Pyr 3 × CH), 7.76 (s, 1 H, NH), 7.58 (s, 1 H, NH), 1.56 (s, 6 H, 2 β-CH_3), 1.38 (s, 12 H, 4 β-CH_3), 1.34 (s, 6 H, 2 β-CH_3) ppm. IR (KBr): $\tilde{\nu}$ = 3284, 1746, 1658, 1635 cm^{-1}.

Pyr–(Aib)$_5$–OH: Yield 87%; m.p. 240–241 °C. R_f1 = 0.10; R_f2 = 0.85; R_f3 = 0.10. ^{1}H NMR (400 MHz, DMSO): δ = 9.15 (s, 1 H, NH), 8.51–8.56 (d, 1 H, Pyr CH), 8.47 (s, 1 H, NH), 8.35–8.38 (d, 2 H, Pyr 2 × CH), 8.32 (s, 1 H, NH), 8.26–8.27 (m, 3 H, Pyr 3 × CH), 8.07–8.25 (m, 3 H, Pyr 3 × CH), 7.61 (s, 1 H, NH), 7.35 (s, 1 H, NH),1.57 (s, 6 H, 2 β-CH_3), 1.42 (s, 6 H, 2 β-CH_3), 1.38 (s, 6 H, 2 β-CH_3), 1.36 (s, 6 H, 2 β-CH_3), 1.34 (s, 6 H, 2 β-CH_3) ppm. IR (KBr): $\tilde{\nu}$ = 3431, 3312, 1738, 1661 cm^{-1}.

Pyr–Aib–NH–TEMPO: Yield 79%; m.p. 228–229 °C (from EtOAc/PE). R_f1 = 0.75; R_f2 = 0.95; R_f3 = 0.20. IR (KBr): $\tilde{\nu}$ = 3373, 1649 cm^{-1}. MS (ESI-TOF): *m*/*z* = 486.32 $[M + H]^+$.

Pyr–(Aib)$_2$–NH–TEMPO: Yield 51%; m.p. 232–233 °C (from EtOAc/PE). R_f1 = 0.55; R_f2 = 0.90; R_f3 = 0.10. IR (KBr): $\tilde{\nu}$ = 3392, 3271, 1687, 1637 cm^{-1}. MS (ESI-TOF): *m*/*z* = 570.35 $[M + H]^+$.

Pyr–(Aib)$_3$–NH–TEMPO: Yield 57%; m.p. 252–253 °C (from EtOAc/PE). R_f1 = 0.55; R_f2 = 0.90; R_f3 = 0.10. IR (KBr): $\tilde{\nu}$ = 3431, 3341, 3281, 1658, 1650 cm^{-1}. MS (ESI-TOF): *m*/*z* = 655.42 $[M + H]^+$.

Pyr–(Aib)$_4$–NH–TEMPO: Yield 72%; m.p. 275–276 °C (from CH_2Cl_2/PE). R_f1 = 0.50; R_f2 = 0.95; R_f3 = 0.10. IR (KBr): $\tilde{\nu}$ = 3433, 3327, 1662 cm^{-1}. MS (ESI-TOF): *m*/*z* = 740.49 $[M + H]^+$.

Pyr–(Aib)$_5$–NH–TEMPO: Yield 71%; m.p. 266–267 °C (from EtOAc/PE). R_f1 = 0.50; R_f2 = 0.95; R_f3 = 0.10. IR (KBr): $\tilde{\nu}$ = 3433, 3326, 1660 cm^{-1}. MS (ESI-TOF): *m*/*z* = 825.57 $[M + H]^+$.

FTIR Absorption: The solution FTIR absorption spectra were recorded with a Perkin–Elmer 1720X spectrophotometer, nitrogen flushed, equipped with a sample-shuttle device, at 2 cm^{-1} nominal resolution, averaging 100 scans. Solvent (base-line) spectra were recorded under the same conditions. Cells with path lengths of 0.1, 1.0, and 10 mm (with CaF_2 windows) were used. Spectrograde $CDCl_3$ (99.8% D) was purchased from Fluka.

^{1}H NMR Spectroscopy: The ^{1}H NMR spectra were recorded with a Bruker AM 400 spectrometer. Measurements were carried out in $CDCl_3$ (99.96% D; Aldrich) and DMSO (99.96% D_6, Acros Organics) with tetramethylsilane as the internal standard. Splitting patterns are abbreviated as follows: (s) singlet, (d) doublet, (t) triplet, (q) quartet; (qd) quartet of doublets, (m) multiplet. Compounds containing the –NH–TEMPO moiety could not be characterized by this technique due to the dramatic line broadening of all signals because of the presence of the paramagnetic nitroxyl group. The 2D ROESY[43,44] experiments were performed with a Bruker AVANCE DRX-400 spectrometer, operating at 400 MHz, equipped with a 5 mm probe BBI-Z grad. Processing of the experimental data was carried out using TOPSPIN 1.3.

Fluorescence: Steady-state fluorescence spectra of the Pyr-containing compounds were carried out with a Perkin–Elmer LS 50B spectrofluorimeter. Cells with path lengths of 1 cm were used. Spectrograde MeOH was purchased from Fluka.

Acknowledgments

F. F. and A. M. are grateful to the University of Padova for financial support (PRAT 2007).

[1] C. Toniolo, E. Benedetti, in: *Molecular Conformation and Biological Interactions* (Eds.: P. Balaram, S. Ramaseshan), Indian Academy of Sciences, Bangalore, India, **1991**, pp. 511–521.
[2] L. Pauling, R. B. Corey, *Proc. Natl. Acad. Sci. USA* **1951**, *37*, 729–740.
[3] A. Åberg, A. Yaremchuk, M. Tukalo, B. Rasmussen, S. Cusack, *Biochemistry* **1999**, *36*, 3084–3094.
[4] M. T. Cung, M. Marraud, J. Néel, *Ann. Chim.* **1972**, *7*, 183–209.
[5] C. Toniolo, *C. R. C. Crit. Rev. Biochem.* **1980**, *9*, 1–44.
[6] M. Crisma, F. Formaggio, C. Toniolo, T. Yoshikawa, T. Wakamiya, *J. Am. Chem. Soc.* **1999**, *121*, 3272–3278.
[7] V. Barone, F. Lelj, A. Bavoso, B. Di Blasio, P. Grimaldi, V. Pavone, C. Pedone, *Biopolymers* **1985**, *24*, 1759–1767.

[8] E. Benedetti, V. Barone, A. Bavoso, B. Di Blasio, F. Lelj, V. Pavone, C. Pedone, G. M. Bonora, C. Toniolo, M. T. Leplawy, K. Kaczmarek, A. Redlinski, *Biopolymers* **1988**, *27*, 357–371.
[9] C. Toniolo, G. M. Bonora, A. Bavoso, E. Benedetti, B. Di Blasio, V. Pavone, C. Pedone, V. Barone, F. Lelj, M. T. Leplawy, K. Kaczmarek, A. Redlinski, *Biopolymers* **1988**, *27*, 373–379.
[10] C. Toniolo, E. Benedetti, *Macromolecules* **1991**, *24*, 4004–4009.
[11] E. Benedetti, B. Di Blasio, V. Pavone, C. Pedone, C. Toniolo, M. Crisma, *Biopolymers* **1992**, *32*, 453–456.
[12] K. Ramnarayan, M. F. Chan, V. N. Balaji, S. Profeta Jr., S. N. Rao, *Int. J. Pept. Protein Res.* **1995**, *45*, 366–376.
[13] M. Cirilli, V. M. Coiro, A. Di Nola, F. Mazza, *Biopolymers* **1998**, *46*, 239–244.
[14] M. Tanaka, N. Imawaka, M. Kurihara, H. Suemune, *Helv. Chim. Acta* **1999**, *82*, 494–510.
[15] M. Kurihara, M. Tanaka, M. Oba, H. Suemune, N. Miyata, in: *Peptides 2000* (Eds.: J. Martinez, J.-A. Fehrentz), EDK, Paris, France, **2001**, pp. 427–428.
[16] C. Toniolo, M. Crisma, F. Formaggio, C. Peggion, *Biopolymers* **2001**, *60*, 396–419.
[17] M. A. C. Preto, A. Melo, S. P. G. Costa, H. L. S. Maia, M. J. Ramos, *J. Phys. Chem. B* **2003**, *107*, 14556–14562.
[18] C. Toniolo, M. Crisma, F. Formaggio, C. Peggion, Q. B. Broxterman, B. Kaptein, *Biopolymers* **2004**, *76*, 162–176.
[19] M. Crisma, F. Formaggio, A. Moretto, C. Toniolo, *Biopolymers* **2006**, *84*, 3–12.
[20] M. Crisma, E. Andreetto, M. De Zotti, A. Moretto, C. Peggion, F. Formaggio, C. Toniolo, *J. Pept. Sci.* **2007**, *13*, 190–205.
[21] J. Torras, D. Zanuy, M. Crisma, C. Toniolo, O. Betran, C. Aleman, *Biopolymers* **2008**, *90*, 695–706.
[22] A. Moretto, M. De Zotti, M. Crisma, F. Formaggio, C. Toniolo, *Int. J. Pept. Res. Ther.* **2008**, *14*, 307–314.
[23] G. R. Marshall, in: *Intra-Science Chemistry Report*, vol. 5 (Ed.: N. Kharasch), Gordon and Breach, New York, **1971**, pp. 305–316.
[24] N. Shamala, R. Nagaraj, P. Balaram, *J. Chem. Soc., Chem. Commun.* **1978**, 996–997.
[25] I. L. Karle, P. Balaram, *Biochemistry* **1990**, *29*, 6747–6756.
[26] G. Jung, H. Brückner, H. Schmitt, in: *Structure and Activity of Natural Products* (Eds.: G. Voelter, G. Weitzel), de Gruyter, Berlin, **1981**, pp. 75–114.
[27] C. Toniolo, E. Benedetti, *Trends Biochem. Sci.* **1991**, *16*, 350–353.
[28] E. Benedetti, C. Pedone, V. Pavone, B. Di Blasio, M. Saviano, R. Fattorusso, M. Crisma, F. Formaggio, G. M. Bonora, C. Toniolo, K. Kaczmarek, A. Redlinski, M. T. Leplawy, *Biopolymers* **1994**, *34*, 1409–1418.
[29] Z. Kaminski, M. T. Leplawy, A. Olma, A. Redlinski, in: *Peptides 1980* (Ed.: K. Brunfeldt), Scriptor, Copenhagen, Denmark, **1981**, pp. 201–206.
[30] M. T. Leplawy, K. Kaczmarek, A. Redlinski, in: *Peptides: Chemistry and Biology* (Ed.: G. R. Marshall), ESCOM, Leiden, The Netherlands, **1988**, pp. 239–241.
[31] W. J. McGahren, M. Goodman, *Tetrahedron* **1967**, *23*, 2017–2030.
[32] L. A. Carpino, *J. Am. Chem. Soc.* **1993**, *115*, 4397–4398.
[33] L. A. Carpino, A. El-Faham, C. A. Minor, F. Albericio, *J. Chem. Soc., Chem. Commun.* **1994**, 201–203.
[34] D. S. Jones, G. W. Kenner, J. Preston, R. C. Sheppard, *J. Chem. Soc.* **1965**, 6227–6239.
[35] E. Benedetti, A. Bavoso, B. Di Blasio, V. Pavone, C. Pedone, M. Crisma, G. M. Bonora, C. Toniolo, *J. Am. Chem. Soc.* **1982**, *104*, 2437–2444.
[36] C. Toniolo, G. M. Bonora, M. Crisma, E. Benedetti, A. Bavoso, B. Di Blasio, V. Pavone, C. Pedone, *Int. J. Pept. Protein Res.* **1983**, *22*, 603–610.
[37] M. T. Leplawy, D. S. Jones, G. W. Kenner, R. C. Sheppard, *Tetrahedron* **1960**, *11*, 39–51.
[38] S. Mizushima, T. Shimanouchi, M. Tsuboi, P. Souda, *J. Am. Chem. Soc.* **1952**, *74*, 270–271.
[39] E. S. Pysh, C. Toniolo, *J. Am. Chem. Soc.* **1977**, *99*, 6211–6219.
[40] C. Toniolo, G. M. Bonora, V. Barone, A. Bavoso, E. Benedetti, B. Di Blasio, P. Grimaldi, F. Lelj, V. Pavone, C. Pedone, *Macromolecules* **1985**, *18*, 895–902.
[41] M. Crisma, A. Moretto, C. Peggion, L. Panella, B. Kaptein, Q. B. Broxterman, F. Formaggio, C. Toniolo, *Amino Acids* **2011**, *41*, 629–641.
[42] N. Imawaka, M. Tanaka, H. Suemune, *Helv. Chim. Acta* **2000**, *83*, 2823–2835.
[43] A. A. Bothner-By, R. L. Stephens, J. Lee, C. D. Warren, R. W. Jeanloz, *J. Am. Chem. Soc.* **1984**, *106*, 811–813.
[44] A. Bax, D. Davis, *J. Magn. Reson.* **1985**, *63*, 207–213.
[45] D. Martin, H. G. Hauthal, in: *Dimethyl Sulphoxide*, van Rostrand-Reinhold, Wokingham, UK, **1975**.
[46] K. D. Kopple, M. Ohnishi, A. Go, *J. Am. Chem. Soc.* **1969**, *91*, 4264–4272.
[47] E. Prasad, K. R. Gopidas, *J. Am. Chem. Soc.* **2000**, *122*, 3191–3196.
[48] M. Sisido, S. Hoshino, H. Kusano, M. Kuragaki, M. Makino, H. Sasaki, T. A. Smith, J. P. Ghiggino, *J. Phys. Chem. B* **2001**, *105*, 10407–10415.
[49] C. Toniolo, M. Crisma, F. Formaggio, *Biopolymers* **1998**, *47*, 153–158.
[50] B. Pispisa, C. Mazzuca, A. Palleschi, L. Stella, M. Venanzi, M. Wakselman, J.-P. Mazaleyrat, M. Rainaldi, F. Formaggio, C. Toniolo, *Chem. Eur. J.* **2003**, *9*, 4084–4093.

Received: August 31, 2011
Published Online: November 16, 2011

